

Edge States in Monolayer and Bilayer Graphene

Wei Li and Ruibao Tao*

Department of Physics, Fudan University, Shanghai, 200433, China

(Dated: January 29, 2010)

The edge states of monolayer and bilayer graphene ribbons both with/without spin-orbit coupling and decoration of edges are studied by means of exact diagonal method. We show that the new extra edge states can be created by the decoration of edge layers. The fundamental picture of the competition among the Rashba, intrinsic spin-orbit coupling (SOC), bias voltage on energy spectrum to effect on the energy spectrum of bilayer graphene and the phase of topological insulators is reported.

PACS numbers: 73.20.At, 71.70.Ej, 61.48.Gh, 68.65.Pq

I. INTRODUCTION

Recently, graphene^{1,2} has greatly attracted multifarious research activities owing to its rich and unexpected phenomena, also its remarkable promise for future nanoelectronics application. It is an unique two dimensional (2D) system with one atomic layer in current physics. Its honeycomb structure provides some unconventional physics behaviors. Different from the usual parabola energy spectrum of excitation in usual semiconductor and Fermi-liquid, the graphene has a Dirac-like linear, massless in low energy spectrum of excitation (up to energies of the order of 1000 K) and the pseudospin degeneracy that make the graphene to be a truly 2D “relativistic” electronic system in solid and can be described by a low energy 2 + 1 dimensional effective massless Dirac theory³⁻⁷ with a Fermi velocity $v_F \approx 10^6 m/s$. Its massless linear energy spectrum presents unconventional physical behaviors such as its Integer Quantum Hall Conductance (IQHC) predicted theoretically⁸⁻¹⁰ and verified experimentally^{11,12}, tunnelling through a potential barrier in graphene¹³ and others. Rather different from 2D Electron Gas (2DEG), graphene has two Dirac points in its Fermion spectrum which are at the Fermi energy for undoped system. In the presence of a perpendicular magnetic field, the energy spectrum of graphene contains positive and negative Landau levels, as well as a zero energy Landau level. It is quite different from the standard 2DEG. Thus IQHC of graphene shows quite different behavior from conventional IQHC^{14,15}. One has known that a wide class of topological phases is tightly related with the existence of edge states. IQHC and Quantum Spin Hall Conductance (QSHC) are two examples¹⁶⁻²⁰. Different from IQHC whose presence fundamentally relies on the breaking of the Time-Reversal Symmetry (TRS) via applied external magnetic field or intrinsic SU(2) gauge flux²¹, TRS is retained in Quantum Spin Hall Effect (QSHE) that ensures the gapless of edge states and robust to non-magnetic disorder owing to Kramers degeneracy. It turns out that a Z_2 -valued topological invariant associates with QSHE^{16,17,22-24}. A theoretical model of graphene with SOC was suggested to explore the topological phase of QSHE by Kane and Mele^{16,17}. In their work, following two kinds of SOC were

introduced:

i). Intrinsic SOC provided from the next nearest neighbor (n.n.n.) spin-dependent hopping term that is something similar to Haldane’s picture²¹. This kind of SOC can generate a bulk energy gap²⁵ and convert graphene from a 2D gapless semiconductor to a topological insulator that presents the QSHE^{16,22} and robust to non-magnetic disorder owing to TRS^{23,27};

ii). Rashba SOC^{22,23,26-29} induced by structure inversion asymmetry. It has been known that QSHE will be gradually destroyed as invasion of the Rashba SOC^{23,25,27}.

However, according to the work by Y. Yao et al.³⁰, the SOC ($10^{-3} meV$) in graphene is much smaller than the one suggested by Kane’s model¹⁶. Therefore the SOC in graphene has been neglected in most works. However, the fundamental picture of QSHE in theoretical model with artificial SOC in graphene and clear understanding the competition among the Rashba, intrinsic SOC and other possible external controllable parameters to effect on the phase of QSHE is very important^{16,31,32}.

In the physics, there might be some correspondence between bulk and edge states in topological states³³ like the IQHC and QSHC, the study of edge states has become a hot topic recently. To study of the edge states of monolayer and bilayer graphene naturally becomes one of the research subjects. It has been found that a non-dispersive zero mode of the edge states (namely a flat band in zero energy) appears in the graphene ribbons (GR) with zigzag edges (GR-ZZE). If the n.n.n. hopping $t' (\approx 0.1t$, here t is the energy of nearest neighbor (n.n.) hopping) is taken into account, its zero mode of the edge states will be changed from the non-dispersive to dispersive^{34,35}. It has been also shown that no edge state exists in GR with armchair edges (GR-ACE).

In bilayer graphene (BG), the spectrum of low energy excitation becomes massive, but it still keeps gapless³⁶. When an electric bias field is applied between two layers of BG, its gapless spectrum can be opened and the gap opened can be tuned by the bias voltage³⁶⁻³⁹. Such transition from gapless to a gapful semiconductor has been observed in experiment³⁹. It was shown that the edge states do exist in BG-ZZE⁴⁰, but not in BG-ACE.

In terms of exact diagonal method, this paper would

give more detail studies on the edge states for monolayer and bilayer graphene ribbons (BGR) with/without SOC as well as the decoration of edges (DE). When the hopping constants connected to the edge sites are chosen as a different value from ones in bulk, it is found that some extra edge states can be created for both GR-ZZE and GR-ACE. It may suggest a way to manipulate the transport behavior of GR by means of decorating the edge layers. In our calculations, we show that different behaviors even both the intralayer Rashba SOC and the interlayer Rashba go against the phase of topological insulators. The invasion of intralayer Rashba SOC in BG reduces the gap in bulk energy spectrum induced by intrinsic SOC down to zero²⁵, but the interlayer Rashba SOC will open a gap for the band of edge states fulfilled in the bulk gap region that drives such topological “edge semimetal” back to be an insulator.

The present paper is organized as follows. In Sec. II, we summarize the results of edge states in graphene with and without DE, but no SOC is considered. The effect of SOC on the energy spectrum, particularly on the edge states, of GR is reported in Sec. III. Sec. IV presents our results on the edge states for BGR. Finally, we give a brief conclusion in sec. V.

II. EDGE STATES IN GR WITHOUT SOC

The electronic transport in graphene is mainly contributed by $p_z - \pi$ orbitals. A tight-binding approximation (TBA) has been well applied and a theoretical model Hamiltonian is

$$\hat{\mathcal{H}}_1 = \sum_{\langle i,j \rangle} t_{ij} c_i^\dagger c_j + \sum_{\ll i,j \gg} t'_{ij} c_i^\dagger c_j + \lambda \sum_i \xi_i c_i^\dagger c_i, \quad (1)$$

where the subscript $\langle i,j \rangle$ in first summation represents a pair of n.n. lattices, $\ll i,j \gg$ in second summation means a pair of the n.n.n. lattices, the hopping constants in bulk are $t_{ij}(=t \approx 2.8\text{eV})$ and $t'_{ij}(=t' \approx 0.1t)$. In our theoretical model, the n.n. hopping constants t_{ij} connected to edge sites are taken as t_0 different from $t(\neq t_0)$ to roughly approach some effective decoration of edges such as the softening of edge structure, atomic substitution and others. The last term in Hamiltonian describes the staggered potential ($\lambda \neq 0, \xi_i = \pm 1$) added on two sublattices that can result the symmetry breaking in exchanging two sublattices A and B. Above Hamiltonian can be diagonalized exactly for ribbons with different edge geometries such as bearded, zigzag and armchair (see Fig. 1(a)). Thus, the eigenvalues and eigenstates can be calculated numerically. Then the energy bands and the local density of states (LDOS) are obtained. In first, we repeat some results again which have been reported in the literatures^{34,35,41–47} for the comparison with our systems having some edge decoration.

Comparing with the bulk energy spectrum of graphene, an extra non-dispersive zero mode of edge state appears

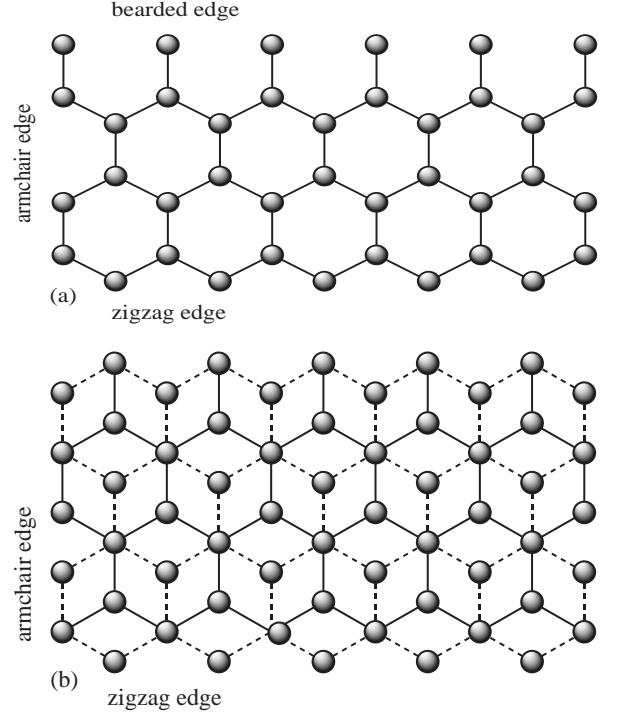


FIG. 1: Schematic illustration of lattice structure of monolayer (a) and bilayer (b) GR.

for zigzag-bearded edged graphene ribbon (GR-ZBE) (see Fig. 1(a)). When the n.n.n. hopping $t' \approx 0.1$ is added, the energy spectrum is shift down and the edge mode in GR-ZBE are changed from the non-dispersive (see Fig. 2(b)) to dispersive (see Fig. 2(d)). In contrast to GR-ZZE and GR-ZBE, no edge state can be found for GR-ACE (see Fig. 2(a)) even n.n.n. hopping is included (see Fig. 2(c)). The basic features in Fig. 2(a) and (c) are qualitatively the same where the linear dispersion near Dirac point $K(K')$ in two cases are still preserved, but a small gap (see Fig. 2(a) and (c)) may appear due to the finite width of the ribbon. The metallic condition of GR-ACE, $n = 3m + 2$, is repeated, here n is chain number and m an integer. The GR-ACE should be an insulator when $n \neq 3m + 2$.

The dispersion relation of the electron spectrum of both GR-ZZE and GR-ACE have been analytically studied based on both continue Dirac equation^{48,49} and discrete model at TBA^{34,35,42–46} with proper boundary conditions. In both zigzag and bearded edged graphene, the zero mode of edge state appears and its wave function vanishes at all sites of one sublattice and localize at another sublattice near the edges of the ribbon. For GR-ACE, no edge state is found. The dispersion relations are shown in Fig. 2(a) and (b) that have been frequently appeared in literatures. For GR-ZZE, the edge states^{34,41,43,45} exist only in region: $2\pi/3 < k_x < 4\pi/3$. However, the edge states exist only in $-2\pi/3 < k_x < 2\pi/3$ for graphene ribbon with bearded-bearded edges

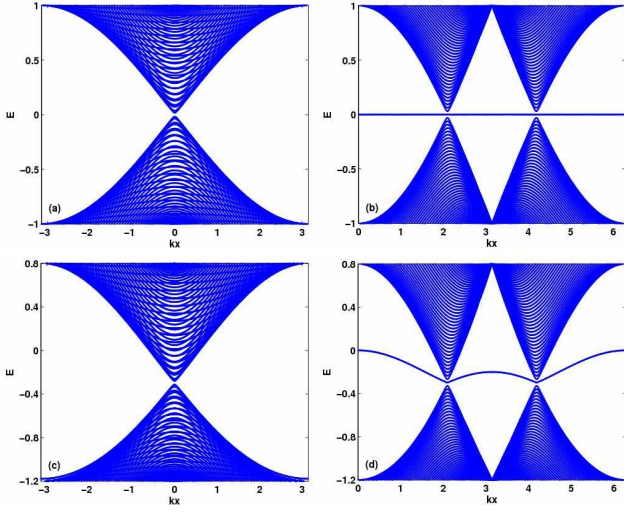


FIG. 2: (color online) The energy spectrum for graphene ribbon with armchair edge (a) and (c), and zigzag-bearded edge (b) and (d). The hopping constants are $t = 1.0, t' = 0$ for (a)-(b), and $t = 1.0, t' = 0.1$ for (c) and (d).

(GR-BBE). Hence, if the GR is zigzag-bearded edged⁴⁵, its edge states will spread to full region of $k_x \in [-\pi, \pi]$ (see Fig. 2(b) and (d)).

When the A - B staggered potential λ is applied, the A - B sublattice symmetry is violated and an bulk energy gap appears (see Fig. 3). The magnitude of gap is approximately proportional to the strength of staggered sublattice potential λ . As we know, if the sublattice at one edge of GR-ZZE or GR-BBE is $A(B)$, the one at another edge of GR must be $B(A)$. But GR-ZBE is different, the type of atoms at two edges must be same. Thus, the energy spectrum of edge states shows something difference that have been shown in Fig. 3.

From the physics, it is able to make some decoration to the atoms near edge surface⁴⁵, here we simply take an effective different hopping constant t_0 in connecting the edge sites to replace the bulk value t . In the case, the spectrum of edge states clearly shows the changes. Some new extra edge states are created when $t_0 \neq t$ (see Fig. 4 and 5). Fig. 4 gives the energy spectrum of GR-ACE with $t_0 \neq t$, where (a), (b), (c) corresponds to $t_0 = 0.2$, $t_0 = 0.5$ and $t_0 = 0.8$, respectively. It is found that some new extra edge states are found at all k_x points across the gap between conducting and valence bands. Changing the ratio t_0/t from 0.2 to 1.0, the new extra edge states are changed dramatically. In the limit of $t_0 = t$, the edge states fully disappear. It may suggest that the edge states can be manipulated by edge decoration. Very similar picture is also obtained for GR-ZZE, GR-BBE and GR-ZBE, some additional edge states also emerge in its energy spectrum (see Fig. 5). The LDOS is attached in Fig. 4(d) and Fig. 5(d) where the LDOS show the exponent decay away from two edges of GR. Fig. 5(a) describes the energy spectrum of the edge states for GR-

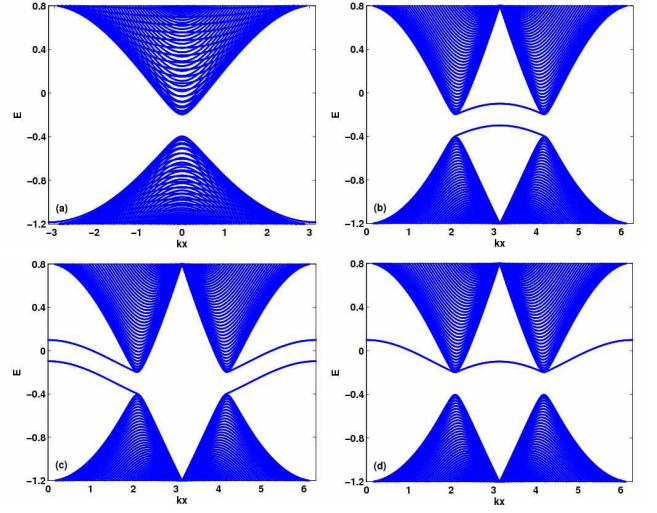


FIG. 3: (color online) The energy spectrum of the graphene ribbon with different edges: (a) armchair-armchair, (b) zigzag-zigzag, (c) bearded-bearded, and (d) zigzag-bearded. All parameters are fixed at $t_0 = t = 1.0, t' = 0.1$ and $\lambda = 0.1$ for (a)-(d).

ZZE with edge decoration where the extra edge states can be found in the rest region of $-2\pi/3 < k_x < 2\pi/3$. Similar feature can be found for GR-BBE with edge decoration from Fig. 5(b) and for GR-ZBE with same edge decoration from Fig. 5(c). The LDOS of edge states are plotted in Fig. 5(d). All extra edge states disappear in the limit of $t_0 \rightarrow t$.

III. EDGE STATES IN GR WITH SOC

Now we turn to study the tight-binding model of graphene with Rashba and intrinsic SOC that was first proposed by Kane and Mele^{16,17}. The model Hamiltonian of the graphene with SOC reads:

$$\begin{aligned} \hat{H}_2 = & \hat{H}_1 + i\lambda_{SO} \sum_{\ll i,j \gg \alpha\beta} \nu_{ij} c_{i\alpha}^\dagger \hat{s}_{\alpha\beta}^z c_{j\beta} \\ & + i\lambda_R \sum_{\langle i,j \rangle \alpha\beta} c_{i\alpha}^\dagger (\hat{s} \times \hat{d}_{ij})_z c_{j\beta}, \end{aligned} \quad (2)$$

where \hat{H}_1 is the free part of hopping terms which has been described in Eq. (1), the second term in Eq. (2) is the intrinsic SOC which is induced by spin-dependent n.n.n. hopping where $\nu_{ij} = (2/\sqrt{3})(\hat{d}_1 \times \hat{d}_2)_z = \pm 1$, (i, j) the index of sites, and (\hat{d}_1, \hat{d}_2) the unit vectors along the two n.n. bonds from site i to j , \hat{s}^z Pauli matrix in z direction. Constant λ_{SO} is the intrinsic SOC and can be estimated in the range from ≈ 0.001 to $\approx 0.05 meV$ in terms of perturbation theory or the first-principles calculations. The third term in Eq. (2) is Rashba SOC induced by a

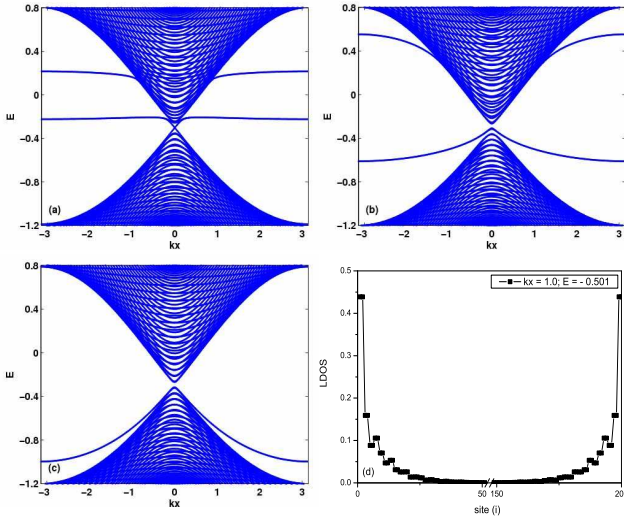


FIG. 4: (color online) The dispersion relation for graphene ribbon with armchair edge (a)-(c) and LDOS (d) corresponding to (b). The parameters: $t = 1.0, t' = 0.1$ for (a)-(c), $t_0 = 0.2$ for (a), $t_0 = 0.5$ for (b), and $t_0 = 0.8$ for (c).

perpendicular electric field and n.n. hopping. The coupling constant λ_R can be experimentally determined by the spin angle-resolved photoemission spectroscopy⁵⁰ or the measurement of spin relaxation^{51,52} in graphene.

The effects of Rashba and intrinsic SOC on energy gap and edge states of the graphene with edge decoration are presented in Fig. 6. From Fig. 6(a), one can see an energy gap and some extra edge states across the gap area where the spin degeneracy has been splitted except the crossing points that is protected by TRS. Thus, it presents a topological insulator which the bulk is insulator, but becomes a metal at surface when an edge is inserted no matter what the geometric structure of edge is, armchair or zigzag edge anyway. Such degeneracy resulted from TRS is robust against non-magnetic disorders^{16,23,27}. If Rashba SOC λ_R exists only, there is no energy gap opened so it is not able to be an insulator. Difference from Rashba SOC, the intrinsic SOC is favorable to induce an energy gap around Dirac point²⁵. More larger λ_{SO} yields more big energy gap (see Fig. 6(d)). When the edge is inserted into bulk, some edge states with spin chiral are created acrossing the gap that results the system to be a metal since the edge states are extended along the edge surface and fulfill the energy gap. Rashba SOC will depress the gap that is unfavorable to the topological phase²⁵. The Fig. 6(d) shows the dependence of gap energy on Rashba SOC λ_R . There is a critical value of λ_R^c above that the energy gap will be closed²⁵.

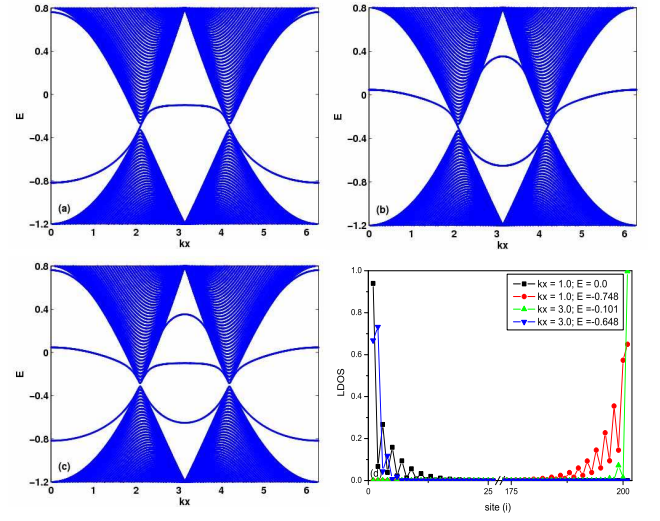


FIG. 5: (color online) (a) is the energy spectrum of graphene ribbons for zigzag-zigzag edge, (b) for bearded-bearded edge, (c) zigzag-bearded edge and (d) for LDOS of the edge states in (c). The parameters are fixed at $t = 1.0, t' = 0.1, t_0 = 0.5$ for (a)-(c).

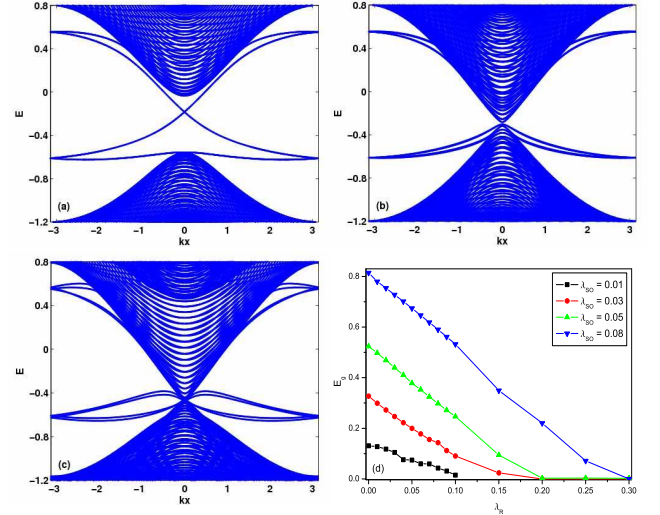


FIG. 6: (color online) The energy spectrum of armchair edged graphene ribbon (a)-(c), and (d) shows energy gap E_g as function of λ_R at different values of λ_{SO} (d). The parameters $\lambda_{SO} = 0.05$ for (a) and (c), $\lambda_R = 0.05$ for (b), and $\lambda_R = 0.2$ for (c).

IV. EDGE STATES IN BGR WITH/WITHOUT SOC

We have mentioned that the Rashba SOC in monolayer graphene contributes a factor to deduce the energy gap²⁵ although intrinsic SOC is favorable for opening an energy gap²⁵. But, it has been known that the gap is very small (zero) in graphene. However, it is reported that the energy gap can be opened in BG by an external electric

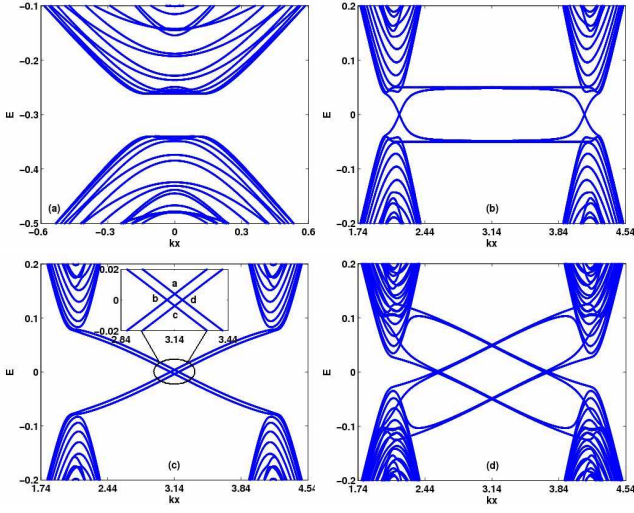


FIG. 7: (color online) The energy spectrum of bilayer graphene ribbons with armchair edge (a) and zigzag edge (b)-(d). The parameters $t = 1$, $t_{\perp} = 0.13$ for (a)-(d), $t' = 0.1$, $t'_{\perp} = 0.11$ for (a), $V_B = 0.1$ for (a), (b) and (d), and $\lambda_{SO} = 0.015$ for (c)-(d).

field³⁶⁻³⁹. In this section, we would study the effect of SOC, bias voltage on the energy spectrum of BGR.

A paper²⁵ reported some results for unbiased and biased bulk systems of bilayer graphene with both the intralayer Rashba and intrinsic SOC as well as an interlayer Rashba SOC. As a result, under certain conditions, the energy spectrum of unbiased BG presents a Mexican hat-like energy dispersion. In the presence of an intralayer Rashba SOC only, another interesting result is that the $K(K')$ point splits into four distinct ones that is contrastive to the case in monolayer graphene where the splitting also takes place, but the low-energy dispersion at these points remains identical.

Here, we focus on the study of edge state for BGR (see Fig. 1b). The Hamiltonian is given by

$$\begin{aligned} \hat{\mathcal{H}} = & \hat{\mathcal{H}}_0 + i\lambda_{SO} \sum_{\langle\langle i,j \rangle\rangle, \alpha\beta\delta} \nu_{ij} c_{i\alpha,\delta}^{\dagger} \hat{s}_{\alpha\beta}^z c_{j\beta,\delta} \\ & + i\lambda_R \sum_{\langle i,j \rangle, \alpha\beta\delta} c_{i\alpha,\delta}^{\dagger} (\hat{s} \times \hat{d}_{ij})_z c_{j\beta,\delta} \\ & + i\lambda_R^{\perp} \sum_{\langle\langle i,j \rangle\rangle, \alpha\beta} c_{i\alpha,1}^{\dagger} (\hat{s} \times \hat{d}_{ij})_z c_{j\beta,2} \\ & + t_{\perp} \sum_{\langle i,j \rangle, \sigma} c_{i\sigma,1}^{\dagger} c_{j\sigma,2} + t'_{\perp} \sum_{\langle\langle i,j \rangle\rangle, \sigma} c_{i\sigma,1}^{\dagger} c_{j\sigma,2} \\ & + \frac{V_B}{2} \sum_{i,\hat{\sigma}} \left(c_{i,\sigma,1}^{\dagger} c_{j,\sigma,1} - c_{i,\sigma,2}^{\dagger} c_{j,\sigma,2} \right) + h.c. \quad (3) \end{aligned}$$

where

$$\hat{\mathcal{H}}_0 = t \sum_{\langle i,j \rangle, \sigma\delta} c_{i\sigma,\delta}^{\dagger} c_{j\sigma,\delta} + t' \sum_{\langle\langle i,j \rangle\rangle, \sigma\delta} c_{i\sigma,\delta}^{\dagger} c_{j\sigma,\delta}.$$

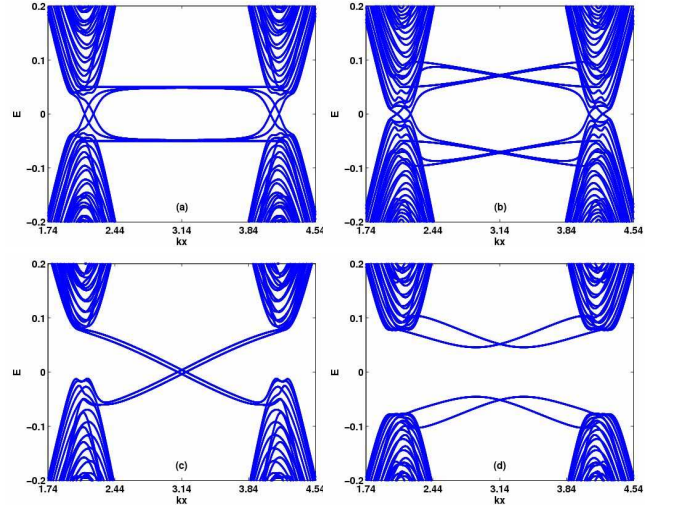


FIG. 8: (color online) The energy spectrum of zigzag edged bilayer graphene ribbon with SOC and bias voltage. The parameters $t = 1$, $t_{\perp} = 0.13$ for (a)-(d), $V_B = 0.1$ for (a) and (b), $\lambda_R = 0.03$ for (a) and (c), $\lambda_R^{\perp} = 0.03$ for (b) and (d), and $\lambda_{SO} = 0.015$ for (c) and (d).

In above equations, we have used the additional subscript σ to denote the spin polarization of electrons ($\sigma = \uparrow, \downarrow$) and δ the layer number ($\delta = 1, 2$). The second and third terms in $\hat{\mathcal{H}}$ are the intrinsic and intralayer Rashba SOC. The fourth term describes n.n.n. interlayer Rashba SOC induced by a bias voltage V_B across two layers of BG, the fifth and sixth terms describe the n.n. and n.n.n. hopping of interlayer⁵³, and the last term is the electric potential yielded by the bias voltage V_B .

In Fig. 7, we give the energy spectrum of the electrons for BGR-ACE (a) and BGR-ZZE (b)-(d). In our precise calculation, it is shown that no edge state can be found in BGR-ACE even for biased case (see Fig. 7(a)). As we have known that linear dispersive spectrum near Dirac point in unbiased BG is changed to be parabolic due to interlayer coupling, but no gap is opened. If a bias field is applied between two layers of BG, a gap will be open in bulk energy spectrum²⁵ (see Fig. 7(a) and (b)). The edge states are found for BGR-ZZE and shown in Fig. 7(b) where two degenerated modes of edge states in two decoupled GR-ZZE now are splitted and mixed due to the interlayer coupling⁴⁰. If the n.n.n. hopping is taken into account, the electron-hole symmetry will be broken. In Fig. 7(c) and (d), the bulk energy gap is opened by intrinsic SOC, and edge states are found in BGR-ZZE. The difference of figure (b) and (c) is that the bulk gap in (b) is induced by bias voltage V_B only, but (c) by the intrinsic SOC only. They show very different feature of edge states. Figure (c) very clearly shows two Dirac cones where the up-down shift of two Dirac cones is from the interlayer coupling. The TRS at crossing points a and c in figure (c) is preserved, but the degeneracy at two crossing points b and d in figure(c) are accidental

and easily splitted by interlayer Rashba SOC λ_R^\perp that is shown in Fig. 8(d). The difference of Fig. 7(c) and Fig. 7(d) shows that further increasing the bias field will reduce the bulk energy gap opened by intrinsic SOC of BGR-ZZE. It is interested that bias voltage is favorable to open bulk energy gap for BGR-ZZE without intrinsic SOC, but becomes unfavorable to keep a gap for the BGR-ZZE system with intrinsic SOC²⁵.

In Fig.8, we report some results on the competition among the Rashba, intrinsic SOC and bias field. We show that both the intralayer and interlayer Rashba SOC can induce the spin polarization and decrease the energy gap (see Fig. 8(a) and (b)), here the bulk energy gap has been opened by bias voltage V_B . The difference of (c) and (d) points out that the interlayer Rashba SOC λ_R^\perp changes the edge states to be gapful. But the Dirac points are still preserved by TRS.

V. CONCLUSIONS

In terms of exact diagonal method, we first report our studies on the edge states for the GR with edge decoration. When the edges of GR has no decoration, perfect boundaries, the edge states exist only for GR-ZZE, GR-ZBE and GR-BBE, but not for GR-ACE, even for biased/unbiased BGR-ACE. However, some extra new

edge states can be created for all GR with decorated edges including GR-ACE. In second, the effects of both the intralayer Rashba and intrinsic SOC on the energy spectrum are studied in detail for GR and BGR. It is shown that the Rashba SOC provides the unfavorable factor to the topological insulator through the deduction of the bulk energy gap. However, the intrinsic SOC drives the graphene to open a gap in the bulk spectrum²⁵, creates the edge states full filled in the gap when an edge is inserted, generates Dirac cones protected by TRS that is favorable to form a topological insulator. At last, we also show that the bias voltage on BG, as same as Rashba SOC, can change the energy spectrum through the deduction of the energy gap. But the interlayer Rashba SOC in BG destroy the topological phase of QSHE through opening the gap in the band of edge state fulfilled in bulk gap region that is also unfavorable to the phase of topological insulator. Thus we conclude that these factors are all not favorable to the formation of the topological insulator except the intrinsic SOC.

Acknowledgments

This work is supported by the National Natural Science Foundation of China under grant No. 10847001 and 973 project of China.

-
- * Electronic address: rbtiao@fudan.edu.cn
- ¹ K. S. Novoselov, A. K. Geim, S. V. Morozov, D. Jiang, Y. Zhang, S. V. Dubonos, I. V. Grigorieva, A. A. Firsov, *Science* **306**, 666 (2004).
 - ² K. S. Novoselov, A. K. Geim, S. V. Morozov, D. Jiang, M. I. Katsnelson, I. V. Grigorieva, S. V. Dubonos, and A. A. Firsov, *Nature* **438**, 197 (2005).
 - ³ P. R. Wallace, *Phys. Rev.* **71**, 622 (1947).
 - ⁴ A. K. Geim and K. Novoselov, *Nature Mater.* **6**, 183 (2007).
 - ⁵ Mikhail I. Katsnelson, *Mater. Today* **10**, 20 (2007).
 - ⁶ A. K. Geim and A. H. MacDonald, *Phys. Today* **60**, 35 (2007).
 - ⁷ A. H. Castro Neto, F. Guinea, N. M. R. Peres, K. S. Novoselov, and A. K. Geim, *Rev. Mod. Phys.* **81**, 109 (2009).
 - ⁸ S. G. Sharapov, V. P. Gusynin, and H. Beck, *Phys. Rev. B* **69**, 075104 (2004).
 - ⁹ V. P. Gusynin and S. G. Sharapov, *Phys. Rev. B* **71**, 125124 (2005).
 - ¹⁰ Masatoshi Sato, Daijiro Tobe, and Mahito Kohmoto, *Phys. Rev. B* **78**, 235322 (2008).
 - ¹¹ Yuanbo Zhang, Yan-Wen Tan, Horst L. Stormer and Philip Kim, *Nature* **438**, 201 (2005).
 - ¹² Yuanbo Zhang, Joshua P. Small, Michael E. S. Amori, and Philip Kim, *Phys. Rev. Lett.* **94**, 176803 (2005).
 - ¹³ M. I. Katsnelson, K. S. Novoselov and A. K. Geim, *Nature Physics* **2**, 620 (2006).
 - ¹⁴ R. E. Prange and S. M. Girvin, *The Quantum Hall Effect* (Springer-Verlag, Berlin, 1990).
 - ¹⁵ D. J. Thouless, M. Kohmoto, M. P. Nightingale, and M. den Nijs, *Phys. Rev. Lett.* **49**, 405 (1982).
 - ¹⁶ C. L. Kane and E. J. Mele, *Phys. Rev. Lett.* **95**, 226801 (2005).
 - ¹⁷ C. L. Kane and E. J. Mele, *Phys. Rev. Lett.* **95**, 146802 (2005).
 - ¹⁸ B. A. Bernevig, T. L. Hughes, and S.-C. Zhang, *Science* **314**, 1757 (2006).
 - ¹⁹ M. Konig, S. Wiedmann, C. Brune, A. Roth, H. Buhmann, L. W. Molenkamp, X.-L. Qi, and S.-C. Zhang, *Science* **318**, 766 (2007).
 - ²⁰ A. Roth, C. Brune, H. Buhmann, L. W. Molenkamp, J. Maciejko, X.-L. Qi, and S.-C. Zhang, *Science* **325**, 294 (2009).
 - ²¹ F. D. M. Haldane, *Phys. Rev. Lett.* **61**, 2015 (1988).
 - ²² Zhigang Wang, Ningning Hao, and Ping Zhang, *Phys. Rev. B* **80**, 115420 (2009).
 - ²³ D.N. Sheng, Z.Y. Weng, L. Sheng, F.D.M. Haldane, *Phys. Rev. Lett.* **97**, 036808 (2006).
 - ²⁴ Shui Murakami, *Prog. Theor. Phys. Suppl.* **176**, 279 (2008).
 - ²⁵ Ralph van Gelderen and C. Morais Smith, arXiv: 0911.0857.
 - ²⁶ Hongki Min, J. E. Hill, N. A. Sinitsyn, B. R. Sahu, Leonard Kleinman, and A. H. MacDonald, *Phys. Rev. B* **74**, 165310, (2006).
 - ²⁷ Zhenhua Qiao and Jian Wang, *Nanotechnology* **18**, 435402 (2007).
 - ²⁸ Mahdi Zarea and Nancy Sandler, *Phys. Rev. B* **79**, 165442 (2009).

- ²⁹ Mahdi Zarea, Nancy Sandler, Physics B: Condensed Matter, **404**, 2694 (2009).
- ³⁰ Yugui Yao, Fei Ye, Xiao-Liang Qi, Shou-Cheng Zhang, and Zhong Fang, Phys. Rev. B **75**, 041401(R) (2007).
- ³¹ L. Sheng, D. N. Sheng, C. S. Ting, and F. D. M. Haldane, Phys. Rev. Lett. **95**, 136602 (2005).
- ³² Daniel Huertas-Hernando, F. Guinea, and Arne Brataas, Phys. Rev. B **74**, 155426 (2006); Phys. Rev. Lett. **103**, 146801 (2009); arXiv: 0811.2171.
- ³³ Y. Hatsugai, arXiv: 0811.1633.
- ³⁴ K. Sasaki, S. Murakami, and R. Saito, Applied Physics Letters **88**, 113110 (2006).
- ³⁵ D. H. Lee and J. D. Joannopoulos, Phys. Rev. B **23**, 4988 (1981).
- ³⁶ Eduardo V. Castro, et al, arXiv: 0807.3348.
- ³⁷ L. A. Falkovsky, arXiv: 0908.3371.
- ³⁸ Jeroen B. Oostinga, Hubert B. Heersche, Xinglan Liu, Alberto F. Morpurgo and Lieven M. K. Vandersypen, nature materials **7**, 151 (2008).
- ³⁹ Eduardo V. Castro, et al. Phys. Rev. Lett. **99**, 216802 (2007).
- ⁴⁰ Eduardo V. Castro, N. M. R. Peres, J. M. B. Lopes dos Santos, A. H. Castro Neto, and F. Guinea, Phys. Rev. Lett. **100**, 026802 (2008).
- ⁴¹ M. Fujita, K. Wakabayashi, K. Nakada and K. Kusakabe, J. Phys. Soc. Jap. **65**, 1920 (1996).
- ⁴² K. Ndkada, M. Fujita, G. Dresselhaus and M. S. Dresselhaus, Phys. Rev. B **54**, 17954 (1996).
- ⁴³ K. Wakabayashi, M. Fujita, H. Ajiki, and M. Sigrist, Phys. Rev. B **59**, 8271 (1999).
- ⁴⁴ Huaixiu Zheng, Z. F. Wang, Tao Luo, Q. W. Shi, and Jie Chen, Phys. Rev. B **75**, 165414 (2007).
- ⁴⁵ Wang Yao, Shengyuan A. Yang, and Qian Niu, Phys. Rev. Lett. **102**, 096801 (2009).
- ⁴⁶ Ken-ichi Sasaki, Yuji Shimomura, Yositake Takane, and Katsunori Wakabayashi, Phys. Rev. Lett. **102**, 146806 (2009).
- ⁴⁷ Jaroslaw Klos, arXiv: 0902.0914.
- ⁴⁸ L. Brey and H. A. Ferting, Phys. Rev. B **73**, 235411 (2006).
- ⁴⁹ A. R. Akhmerov and C. W. J. Beenakker, Phys. Rev. B **77**, 085423 (2008).
- ⁵⁰ A. Varykhalov, J. Sanchez-Barriga, A. M. Shikin, C. Biswas, E. Vescovo, A. Rybkin, D. Marchenko, and O. Rader, Phys. Rev. Lett. **101**, 157601 (2008).
- ⁵¹ N. Tombros, C. Jozsa, M. Popinciuc, H. T. Jonkman, and B. J. van Wees, Nature **448**, 571 (2007).
- ⁵² N. Tombros, S. Tanabe, A. Veligura, C. Jozsa, M. Popinciuc, H. T. Jonkman, and B. J. van Wees, Phys. Rev. Lett. **101**, 046601 (2008).
- ⁵³ R. Ma, L. J. Zhu, L. Sheng, M. Liu, D. N. Sheng, Europhys. Lett. **87**, 17009 (2009).